Proton ionization of the L subshells of Pr, Eu, Gd, and Dy: 0.3 to 2.0 MeV†

F. Abrath and Tom J. Gray
Department of Physics, North Texas State University, Denton, Texas 76203
(Received 4 February 1974)

Total L-shell ionization cross sections were measured for Pr, Eu, Gd, and Dy over the energy range 0.3–0.2 MeV and compared to the nonrelativistic plane-wave Born approximation (PWBA), the constrained binary-encounter approximation (CBEA), and the binary-encounter approximation. Both the PWBA and CBEA predicted the measured values. Also the $L\alpha_{1,2}/Ll$, $L\alpha_{1,2}/L\gamma_1$, $L\alpha_{1,2}/L\gamma_{2,3}$, and $L\gamma_1/L\gamma_{2,3}$ ratios were measured and compared with PWBA and CBEA. The results showed that the CBEA and PWBA accurately predicted the $L_{\rm II}$- and $L_{\rm III}$-subshell ionization cross sections, while only the PWBA accurately predicted the $L_{\rm I}$-subshell ionization cross section.

I. INTRODUCTION

Ion-induced L-shell x-ray production cross sections and x-ray ratios have been studied recently by several authors.[1-4] A previous paper by the present authors[5] studied the $L\gamma_1/L\gamma_{2,3}$, $L\alpha_{1,2}/L\gamma_{2,3}$, $L\alpha_{1,2}/L\gamma_1$, and $L\alpha_{1,2}/Ll$ ratios for 0.3–2.0-MeV protons on samarium. The data were compared with the nonrelativistic Born approximation (PWBA)[6] and the constrained binary-encounter approximation (CBEA)[7] in an attempt to understand the energy dependence of the $L_{\rm I}$-, $L_{\rm II}$-, and $L_{\rm III}$-subshell ionization cross sections. The PWBA most correctly predicted the peak position, height, and shape of the $L\alpha_{1,2}/L\gamma_{2,3}$ and $L\gamma_1/L\gamma_{2,3}$ ratios taken as a function of proton energy. From this it was concluded that the PWBA most correctly predicts the $L_{\rm I}$-, $L_{\rm II}$-, and $L_{\rm III}$-subshell ionization cross sections, while the CBEA predicts the $L_{\rm II}$- and $L_{\rm III}$-ionization cross sections, but incorrectly predicts the $L_{\rm I}$-ionization cross sections. The present paper presents a further study of the L-subshell process for protons on Pr, Eu, Gd, and Dy. The measured ratios are compared to the predictions of the nonrelativistic PWBA and CBEA. Also total L-shell ionization cross sections for these elements were measured and compared to the PWBA, CBEA, and BEA.[8]

II. EXPERIMENTAL PROCEDURE

As described in Ref. 5 the protons accelerated by a 2-MeV Van de Graaff were incident on thin targets mounted at 45° to the beam. The targets were made by standard evaporation techniques on thin carbon foils. The target thicknesses used in this work were 12.2 (Pr), 37.4 (Eu), 9.4 (Gd), and 22.4 μg/cm^2 (Dy). A Si(Li) detector with a resolution of 168 eV at 5.898 keV was mounted at 90° to the beam outside the vacuum system separated by a 0.25-mm Mylar window. The efficiency of the x-ray detector was measured using the methods described by Gehrke and Lokken,[9] Hansen *et al.*,[10] and Lear and Gray.[11] The backscattered protons were detected by a surface barrier detector mounted at 168° to the beam and used to monitor the thickness of the targets. The x-ray spectra were fitted by a modified version of the program SAMPO.[12]

III. RESULTS AND DISCUSSION

A. Total L-shell ionization cross sections

Total L-shell ionization cross section data are tabulated in Table I and plotted in Fig. 1 with the predictions of the PWBA, CBEA, and BEA. Also listed in Table I are the thick-target results of Khan, Potter, and Worley.[13] The measurements in the laboratory give x-ray production cross sections not ionization cross sections. The relationship between the ionization cross section ($\sigma_{\rm I}$) and the x-ray production cross section [σ_L(x ray)] is $\sigma_{\rm I} = \sigma_L(\text{x ray})/\omega_L$, where ω_L is the average L-shell fluorescence yield. The values of the ω_L's were taken from Bambynek *et al.*[14] and were 0.167, 0.17, 0.198, and 0.210 for Pr, Eu, Gd, and Dy, respectively. As can be seen from Fig. 1 the CBEA and the PWBA yield almost identical theoretical values for all four elements above 1.0 MeV, but below 1.0 MeV the CBEA begins dropping below the PWBA. However, both the CBEA and PWBA predict the cross sections within the error bars of the data throughout the entire energy range for Eu, Gd, and Dy. For Pr the CBEA and PWBA are only slightly higher than the data. The BEA is 15–40% lower than the data for Dy, Gd, and Eu but predicts the general shape of the measured cross sections. For Pr the BEA is within the error bars for energies above 1.0 MeV, but below 1.0 MeV the BEA is again lower than the data.

B. L-subshell cross sections

Although the predictions of the PWBA and CBEA for the total L-shell ionization cross sections agree quite well with the data presented here, it was shown in a previous paper[5] that the predictions of these two theories disagree for the L_{I}-subshell ionization cross sections but agree reasonably well for the L_{II}- and L_{III}-subshell ionization cross sections. The difference in the predictions of the L_{I}-subshell ionization cross section is in the energy dependence. The CBEA predicts a smooth function for $\sigma_{L_{\mathrm{I}}}$, whereas the PWBA prediction has more structure.

In order to relate the theoretical predictions to the measured x-ray cross sections the following expressions are used:

$$\sigma_{L\alpha_{1,2}} = [\sigma_{L_{\mathrm{III}}} + f_{23}\sigma_{L_{\mathrm{II}}} + (f_{12}f_{23} + f_{13})\sigma_{L_{\mathrm{I}}}] \times \omega_3(\Gamma_{3\alpha_1} + \Gamma_{3\alpha_2})/\Gamma_3 ,$$

$$\sigma_{L\gamma_1} = (\sigma_{L_{\mathrm{II}}} + f_{12}\sigma_{L_{\mathrm{I}}})\omega_2\Gamma_{2\gamma_1}/\Gamma_2 ,$$

$$\sigma_{L\gamma_{2,3}} = \sigma_{L_{\mathrm{I}}}\omega(\Gamma_{1\gamma_2} + \Gamma_{1\gamma_3})/\Gamma_1 .$$

The f_{ij}'s are the Coster-Kronig yields obtained from McGuire.[15] The Γ_i's are the radiative widths taken from Scofield.[16] The ω_i's are the subshell fluorescence yields. The values of ω_1 were taken from Crasemann, Chen, and Kostroun,[17] and the values of ω_2 and ω_3 were taken from Chen, Crasemann, and Kostroun.[18] The σ_i's were taken from the nonrelativistic theory of Choi, Merzbacher,

TABLE I. Total experimental L-shell cross sections (in barns).

Element	Proton energy (MeV)	$\sigma_{(\text{x ray})}$ this work	$\sigma_{(\text{x ray})}$ previous work (Ref. 13)	σ_{I} this work
Pr, $\bar{\omega}_L = 0.17$	0.3	2.5±0.2		15±1
	0.4	7.1±0.7		42±4
	0.5	13±1		78±8
	0.6	21±2		127±13
	0.7	32±3		191±19
	0.8	44±4		263±26
	0.9	54±5		326±33
	1.0	66±7		395±39
	1.1	84±8		504±50
	1.2	96±10		575±57
	1.3	122±12		732±73
	1.4	137±14		820±82
	1.5	156±16		937±94
	1.6	175±17		1050±100
	1.7	205±20		1230±120
	1.8	213±21		1280±130
	1.9	227±23		1360±140
	2.0	258±26		1540±150
Eu, $\bar{\omega}_L = 0.17$	0.5	7.1±0.7		42±4
	0.6	12.0±1.0		70±7
	0.7	17.1±2.0		100±11
	0.8	23.4±2.4		138±15
	0.9	30.9±3.3		182±18
	1.0	37.9±4.0		223±23
	1.1	46.7±5.1		275±28
	1.2	59.4±6.2		349±36
	1.3	69.6±7.3		409±42
	1.4	82.4±8.5		485±50
	1.5	95.3±9.8		561±58
	1.6	108±13		637±65
	1.7	121±13		713±72
	1.8	139±15		817±82
	1.9	146±16		859±87
	2.0	168±17		987±99
Gd, $\bar{\omega}_L = 0.19$	0.5	7.3±0.8	4.2	37±4.0
	0.6	12.1±1.0		61.1±6.1
	0.7	18.0±2.0	10	90.2±10.0
	0.8	25.3±2.8		128±13
	0.9	33.1±3.6	20	166±17
	1.0	41.6±4.4		210±22
	1.1	51.5±5.3	32	257±27
	1.2	62.3±6.4		313±33
	1.3	76.4±7.8	46	381±40
	1.4	82.3±8.4		451±42
	1.5		61	
	1.6	114±13		579±59
	1.7	122±14	80	615±63
	1.8	140±15		712±73
	1.9	164±17		831±85
	2.0	170±18		859±88
Dy, $\bar{\omega} = 0.21$	0.3	0.9±0.1		4.3±4
	0.4	2.6±0.3		12±1
	0.5	5.4±0.6	2.9	26±3
	0.6	9.0±0.9		43±4
	0.7	14.0±1.6	8.3	66.1±6.8
	0.8	19.3±2.1		93.2±9.4
	0.9	26.1±2.8	16	126±13
	1.0	34.4±3.6		162±18
	1.1	43.4±4.6	26	204±22
	1.2	52.1±5.4		249±26
	1.3	62.3±6.5	38	299±31
	1.4	69.1±7.1		329±34
	1.5	83.8±8.5	52	402±42
	1.6	100±11		474±49
	1.7	112±13	70	533±60
	1.8	123±13		584±60
	1.9	129±14		617±63
	2.0	159±17		759±77

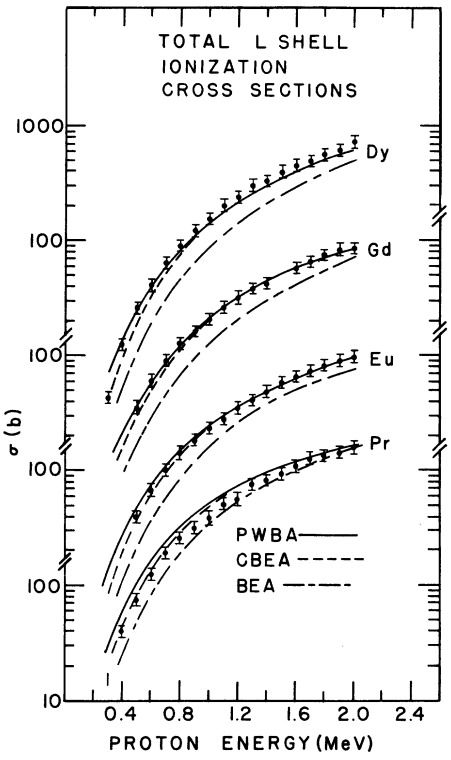

FIG. 1. Measured values of total L-shell ionization cross sections for Pr, Eu, Gd, and Dy compared with the predictions of the PWBA, CBEA, and BEA.

and Khandelwal,[6] and the CBEA by Hansen.[7] The theoretical cross section ratios, $L\gamma_1/L\gamma_{2,3}$, $L\alpha_{1,2}/L\gamma_{2,3}$, and $L\alpha_{1,2}/L\gamma_1$, are then compared with the experimental ratios.

Shown in Fig. 2 are the relative intensity measurements for $L\alpha_{1,2}/L\gamma_{2,3}$ and the theoretical predictions of the PWBA and the CBEA. These experimental ratios are listed in Table II. The PWBA predicts the correct shape and peak position for all four elements, fitting within the error bars for Dy, Gd, and Eu, and being only slightly above the data for Pr. The CBEA, however, predicts the peak at a higher energy (approximately 0.5 MeV in each case) and is clearly not as sharply peaked as the data. Also from Fig. 2 it can be seen that the peak position increases in energy with increasing Z: from $E_p = 0.6$ for $Z = 59$ to $E_p = 0.9$ for $Z = 66$. Both the theories exhibit this increase in the peak position with atomic number.

Plotted in Fig. 3 are the experimental data and theoretical predictions for the $L\gamma_1/L\gamma_{2,3}$ ratios. The experimental ratios are listed in Table III. As in the case of the $L\alpha_{1,2}/L\gamma_{2,3}$ ratios the PWBA affords an excellent fit to the data, falling within the error bars for all four elements. The CBEA again predicts the peak position about 0.5 MeV too high and predicts a less sharply peaked structure. It is again noted that the data peaks at a proton energy that increases with Z. Again this Z dependence is predicted by both theories. In comparing

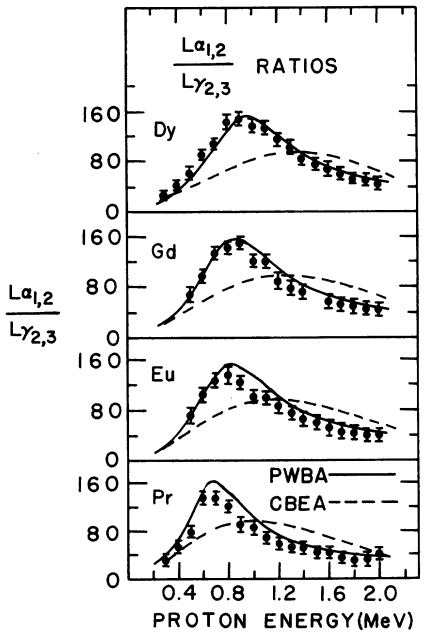

FIG. 2. Measured values of $L\alpha_{1,2}/L\gamma_{2,3}$ ratios for Pr, Eu, Gd, and Dy compared with the predictions of the PWBA and CBEA.

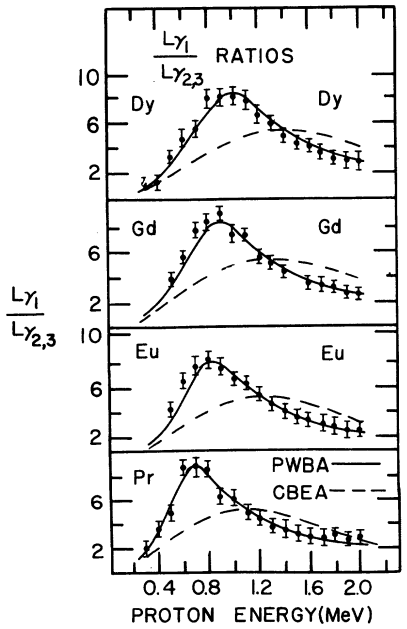

FIG. 3. Measured values of $L\gamma_1/L\gamma_{2,3}$ ratios for Pr, Eu, Gd, and Dy compared to the predictions of the PWBA and CBEA.

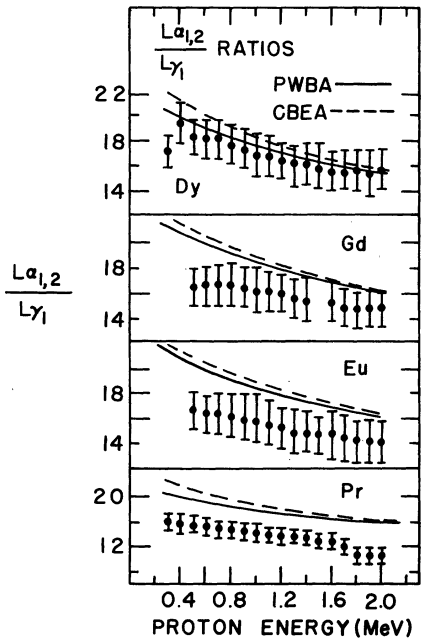

FIG. 4. Measured values of the $L\alpha_{1,2}/L\gamma_1$ ratios for Pr, Eu, Gd, and Dy compared to the predictions of the PWBA and CBEA.

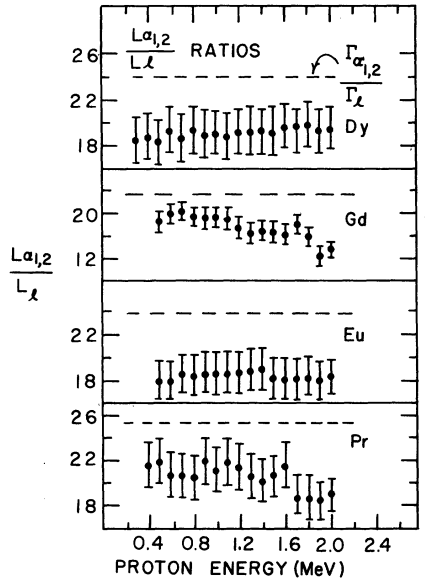

FIG. 5. Measured values of the $L\alpha_{1,2}/L_l$ ratios compared with the radiative-width predictions of Scofield (Ref. 16).

the PWBA fit for the $L\gamma_1/L\gamma_{2,3}$ ratios for these four elements to the previous work[5] done on samarium it must be noted that in the previous work the values used for the ω_i's were taken from McGuire. The values for ω_i's in this work are slightly lower than McGuire's values accounting for the lower theoretical predictions than in the samarium work.

Plotted in Fig. 4 are the experimental values and theoretical predictions of the $L\alpha_{1,2}/L\gamma_1$ ratios. The experimental ratios are listed in Table IV. In this case both the PWBA and CBEA predict the general shape of the data. For dysprosium the theories fit within the error bars, while for gadolinium and europium the theories are approximately 10–15% above the data throughout the energy range. For praseodymium the theories are approximately 25% higher than the data throughout the energy range. The experimental data for the $L\alpha_{1,2}/L_l$ ratios are recorded in Table V and plotted in Fig. 5. Because both the $L\alpha_{1,2}$ and L_l x rays are representative of transitions to the same subshell ($L_{\rm III}$) it is expected that the ratios should be

TABLE II. $L\alpha_{1,2}/L\gamma_{2,3}$ ratios.

Energy (MeV)	Pr	Eu	Gd	Dy
0.3	34.0±4.8			23.6±3.3
0.4	58.1±8.2			40.0±5.6
0.5	74.3±10.5	72.2±10.2	66.4±9.4	61.4±8.7
0.6	137±19	108±15	97.1±13.7	88.9±12.6
0.7	134±19	128±18	132±19	106±15
0.8	126±18	136±19	139±20	144±20
0.9	91.8±13.0	123±17	150±21	143±20
1.0	85.0±12.0	109±15	120±17	135±19
1.1	66.7±9.4	97.6±13.8	120±17	133±19
1.2	58.4±8.2	85.2±12.0	92.2±13.0	110±15
1.3	53.7±7.6	72.7±103	78.9±11.1	100±14
1.4	49.4±6.9	63.5±9.0	70.4±9.9	81.8±11.5
1.5	41.6±5.9	57.6±8.1		71.4±10.1
1.6	39.5±5.6	53.0±7.5	54.0±7.6	67.3±9.5
1.7	34.0±4.8	46.6±6.6	49.8±7.0	58.1±8.2
1.8	33.8±4.8	42.7±6.0	47.2±6.7	52.1±7.4
1.9	30.1±4.2	40.3±5.7	41.9±5.9	48.3±6.8
2.0	31.6±4.5	38.2±5.4	40.1±5.7	48.5±6.8

TABLE III. $L\gamma_1/L\gamma_{2,3}$ ratios.

Energy (MeV)	Pr	Eu	Gd	Dy
0.3	2.17±0.31			1.37±0.19
0.4	3.77±0.53			1.30±0.98
0.5	4.90±0.69	4.32±0.61	4.02±0.57	3.45±0.49
0.6	8.90±1.25	6.63±0.94	5.83±0.82	4.90±0.69
0.7	9.10±1.29	7.84±1.11	7.96±1.12	5.76±0.81
0.8	8.74±1.24	8.43±1.19	8.48±1.19	8.13±1.15
0.9	6.29±0.89	7.71±1.09	9.25±1.31	8.24±1.16
1.0	6.12±0.86	6.86±0.97	7.48±1.05	8.10±1.14
1.1	4.96±0.70	6.35±0.90	7.44±1.05	7.88±1.11
1.2	4.34±0.61	5.59±0.79	5.76±0.81	6.71±0.95
1.3	3.94±0.56	4.88±0.69	5.10±0.72	6.15±0.87
1.4	3.65±0.52	4.29±0.61	4.53±0.64	5.00±0.71
1.5	3.30±0.47	3.89±0.55		4.49±0.63
1.6	3.09±0.44	3.59±0.51	3.53±0.50	4.35±0.61
1.7	3.09±0.44	3.25±0.46	3.60±0.45	3.32±0.47
1.8	3.25±0.46	3.02±0.43	3.20±0.45	3.32±0.47
1.9	2.90±0.41	2.86±0.40	2.82±0.40	3.20±0.45
2.0	3.12±0.44	2.73±0.39	2.71±0.38	3.15±0.44

TABLE IV. $L\alpha_{1,2}/L\gamma_1$ ratios.

Energy (MeV)	Pr	Eu	Gd	Dy
0.3	16.0±2.3			17.2±2.4
0.4	15.5±2.2			19.3±2.7
0.5	15.2±2.1	16.7±2.4	16.5±2.3	18.1±2.5
0.6	15.4±2.2	16.3±2.3	16.6±2.3	18.1±2.5
0.7	14.8±2.1	16.4±2.3	16.6±2.3	18.4±2.6
0.8	14.4±2.0	16.1±2.3	16.5±2.3	17.7±2.5
0.9	14.6±2.1	15.9±2.2	16.2±2.3	17.3±2.4
1.0	13.9±2.0	15.8±2.2	16.0±2.3	16.7±2.4
1.1	13.4±1.9	15.4±2.2	16.1±2.3	16.9±2.4
1.2	13.5±1.9	15.2±2.1	16.0±2.3	16.4±2.3
1.3	13.6±1.9	14.9±2.1	15.4±2.2	16.3±2.3
1.4	13.5±1.9	14.8±2.1	15.6±2.2	16.3±2.3
1.5	12.6±1.8	14.8±2.1		15.9±2.2
1.6	12.7±1.8	14.7±2.1	15.3±2.2	15.5±2.2
1.7	11.1±1.6	14.3±2.0	14.8±2.1	15.3±2.2
1.8	10.4±1.5	14.1±2.0	14.7±2.1	15.7±2.2
1.9	10.4±1.5	14.1±2.0	14.8±2.1	15.1±2.1
2.0	10.1±1.4	14.0±2.0	14.8±2.1	15.4±2.2

TABLE V. Experimental $L\alpha_{1,2}/Ll$ ratios.

E_p (MeV)	Pr	Eu	Gd	Dy
0.3				17.2±2.4
0.4	21.6±3.0			18.8±2.6
0.5	22.0±3.1	18.0±2.5	18.6±2.6	18.3±2.6
0.6	20.8±2.9	18.0±2.5	20.0±2.8	19.3±2.7
0.7	20.7±2.9	18.7±2.6	20.8±2.9	18.6±2.6
0.8	20.5±2.9	18.4±2.6	19.5±2.7	19.4±2.7
0.9	22.1±3.1	18.7±2.6	19.1±2.7	18.9±2.7
1.0	20.9±2.9	18.5±2.6	19.4±2.7	19.1±2.7
1.1	21.8±3.1	18.6±2.6	17.8±2.5	18.9±2.7
1.2	21.4±3.0	18.7±2.6	17.8±2.5	19.2±2.7
1.3	20.6±2.9	18.9±2.7	17.1±2.4	19.2±2.7
1.4	20.1±2.8	19.1±2.7	17.6±2.5	19.3±2.7
1.5	20.8±2.9	18.3±2.6		19.2±2.7
1.6	21.6±3.0	18.2±2.6	16.5±2.3	19.6±2.8
1.7	18.8±2.6	18.1±2.5	18.2±2.6	19.2±2.7
1.8	18.8±2.6	18.3±2.6	16.4±2.3	19.8±2.8
1.9	18.2±2.6	17.5±2.5	13.3±1.9	19.2±2.7
2.0	18.7±2.7	18.4±2.6	13.9±2.0	19.4±2.7

constant. Theoretically the $L\alpha_{1,2}/Ll$ ratios are predicted as the ratios of $\Gamma_{3\alpha_{1,2}}$ to Γ_{3l} as predicted by Scofield.[16] The experimental data generally fall in a straight line about 20% below the theory for Dy, Eu, and Pr and approximately 20–50% below the theory for Gd.

IV. CONCLUSION

This work shows that for protons in the energy range 0.3–2.0 MeV on Pr, Eu, Gd, and Dy both the PWBA and CBEA reproduce the total L-shell ionization cross sections very closely in magnitude and structure. The BEA predicts values for σ_I that are generally 15–45% lower than the data but having a shape quite consistent with the experimental cross sections.

The CBEA and PWBA both yield consistent theoretical results in their predictions of the $L\alpha_{1,2}/L\gamma_1$ ratios. This ratio is most strongly dependent on the L_{II}- and L_{III}-subshell ionization cross sections. Both the CBEA and PWBA describe the L_{II}- and L_{III}-subshell cross sections adequately. The $L\alpha_{1,2}/L\gamma_{1,2}$ and $L\gamma_1/L\gamma_{2,3}$ ratios strongly depend on the L_I-subshell ionization cross section. Because the PWBA fits these measured ratios accurately while the CBEA does not, it must be concluded that the quantum-mechanical approach to calculating the L_I-subshell ionization cross sections (the PWBA) is a better method than the classical-physics approach (the CBEA).

ACKNOWLEDGMENTS

The authors wish to thank Dr. B.-H. Choi for providing the PWBA calculations and Dr. J. S. Hansen for providing the computer code for the CBEA calculations. We also wish to thank G. Pepper for many helpful discussions and critical comments on this work.

†Work supported in part by the Faculty Research Fund, North Texas State University, Denton, Texas 76203.

[1]S. M. Shafroth, G. A. Bissinger, and A. W. Waltner, Phys. Rev. A 7, 566 (1973).
[2]G. A. Bissinger, A. B. Baskin, B.-H. Choi, S. M. Shafroth, J. M. Howard, and A. W. Waltner, Phys. Rev. A 6, 545 (1972).
[3]C. E. Busch, A. B. Baskin, P. H. Nettles, S. M. Shafroth, and A. W. Waltner, Phys. Rev. A 7, 1601 (1973).
[4]D. A. Close, R. C. Bearse, J. J. Malanify, and C. J. Umbarger, Phys. Rev. A 8, 1873 (1973).
[5]F. Abrath and T. J. Gray, Phys. Rev. A 9, 682 (1974).
[6]B.-H. Choi, E. Merzbacher, and G. S. Khandewal, At. Data 5, 291 (1973).
[7]J. S. Hansen, Bull. Am. Phys. Soc. 18, 663 (1973).
[8]J. D. Garcia, E. Gerjuoy, and J. E. Welker, Phys. Rev. 165, 66 (1967).
[9]R. J. Gehrke and R. A. Lokken, Nucl. Instrum. Meth. 97, 219 (1971).
[10]J. S. Hansen, J. C. McGeorge, D. Nix, W. D. Schmidt-Ott, I. Unus, and R. W. Fink, Nucl. Instrum. Meth. 106, 365 (1973).
[11]R. Lear and Tom J. Gray, Phys. Rev. A 8, 2469 (1973).
[12]J. T. Routti and S. G. Prussin, Nucl. Instrum. Meth. 72, 125 (1969).
[13]J. M. Kahn, D. L. Potter, and R. D. Worley, Phys. Rev. 139, A1735 (1965).
[14]W. Bambynek, B. Crasemann, R. W. Fink, H. V. Freund, H. Mark, C. D. Swift, R. E. Price, and P. Venugopala Rao, Rev. Mod. Phys. 44, 716 (1972).
[15]E. J. McGuire, Phys. Rev. A 3, 587 (1971).
[16]J. H. Scofield, Phys. Rev. 179, 9 (1969).
[17]B. Crasemann, M. H. Chen, and V. O. Kostroun, Phys. Rev. A 4, 2161 (1971).
[18]M. H. Chen, B. Crasemann, and V. O. Kostroun, Phys. Rev. A 4, 1 (1971).